Application of Tensor Decomposition in Removing Motion Artifacts from the Measurements of a Wireless Electrocardiogram

Jannis Lilienthal and Waltenegus Dargie
Technische Universität Dresden
01062 Dresden, Germany
{jannis.lilienthal, waltenegus.dargie}@tu-dresden.de

***Abstract*—Wireless electrocardiograms (WECG) facilitate the long-term monitoring of patients in their residential environment. However, the freedom of movement provokes motion artifacts in the measurements of the useful signals, which significantly affect the quality of the data. In this paper, we propose a tensor decomposition method to combine data from heterogeneous sources and remove motion artifacts. We transformed synchronously sampled electrocardiogram and inertial sensors into the time-frequency space using wavelet decomposition. Afterward, we formed a three-way tensor consisting of a single lead WECG and a motion reference. Thus we recorded measurements from eleven healthy subjects undertaking different types of movements, namely, *Standing up*, *Bending forward*, *Walking*, *Running*, *Jumping*, and *Climbing stairs*. An additional WECG sensor was attached at the back of each subject to measure motion with negligible cardiac input. This signal was subsequently added to a noise-free WECG segment to generate artificially corrupted signal. We factorize the measurement sets using Canonical Polyadic Decomposition to determine mutual information present in both sensor types (WECG and inertial sensor) and extract the motion artifacts from the noisy WECG. We evaluated the results by considering the Signal-to-Noise-Ratio and the Root Mean Squared Error between the actual and estimated artifacts.**

***Index Terms*—Inertial sensors, motion artifact, telemedicine, tensor decomposition, wireless electrocardiogram**

I. Introduction

The most recent statistics published by the World Health Organization (WHO) reveal that cardiovascular diseases (CVD) remain the leading cause of death worldwide. Every year 17.9 million people die from CVDs, an estimated 31% of all deaths worldwide [1].

Early diagnosis is essential to start the appropriate treatment for patients and reduce the risk of mortality. The electrocardiogram (ECG) is the most frequently used method to detect cardiac arrhythmia. It measures the hearts' activity on the surface of the body and provides insights into pathological symptoms that would otherwise remain hidden. As late diagnosis can lead to severe complications and hinder effective treatments, the availability of portable and reliable ECG devices is crucial. Wireless electrocardiograms provide a user-friendly opportunity to observe the patients' cardiac activity continuously. With a decrease in cost and size, wearable devices increasingly facilitate the monitoring of daily activities. However, monitoring patients in their residential environment comes with a downside. The wireless ECG is easily affected by the movement of patients, which can significantly distort the signal. These artifacts hinder an accurate interpretation of the ECG, and their removal remains a challenging task. Traditional frequency filters fail to adequately eliminate them as the spectrum of the useful cardiac activity and motion overlap in their frequency range [2]. The effect of motion artifacts on the ECG is manifold and can lead, among others, to higher false-positive QRS detections [3].

Previously, many approaches have been presented to remove motion artifact from the electrocardiogram: Independent Component Analysis [4], [5], Adaptive Filter [6]–[8], Wavelet Transformation [9]–[11], Tensor Decomposition [12] and a combination of these [13]–[15]. In this paper, we propose a dimensionality reduction technique to combine ECG data with motion reference sensors and remove artifacts from the electrocardiogram. Therefore, we recorded a series of WECG while the subjects undertake different types of everyday activities. Simultaneously, we measured physical exertion by employing inertial sensors and combined the measurements in a multi-dimensional array and apply tensor decomposition in order to remove motion artifacts from the measurements.

We organize the remaining part of this paper as follows: In section II, we review related work. In section III we give a brief introduction to data factorization. In section IV, we describe the experimental setup and the applied tensor decomposition to combine sensors and remove motion artifacts. In section V, we evaluate the results of the proposed artifact reduction technique. Closing with section VI, we conclude our work and state open issues that we wish to target in future research.

II. Related Work

The following review of related work focuses on the multi-dimensional decomposition techniques and their application to bio-medical signals as well as approaches employing reference sensors. For a more comprehensive survey on practices and possibilities for artifact removal in physiological signals, we refer the reader to the following review [16].

The application of adaptive filtering covers a wide range using a variety of reference sensors. Tong et al. [8] employ two

This work has been funded by the German Research Foundation (DFG) under the project agreement: DA 1211/7-1 (RoReyBaN)

accelerometers mounted on ECG electrodes to reduce motion artifacts in the electrocardiogram by feeding the accelerometer data to the adaptive filter algorithm. Liu et al. [17] measure the skin stretch by employing a non-invasive light-emitting diode and an optical sensor integrated into the ECG electrodes. The sensor readouts were subsequently used as motion reference in a Least-Mean Squares (LMS) adaptive filter. Romero et al. [18] compare the performance of adaptive filters using an accelerometer and the skin-electrode impedance as reference signals. Ghaleb et al. [19] combine a weighted adaptive noise canceling with a recursive Hampel filter.

Kirst et al. [3] apply the Discrete Wavelet Transform (DWT) on the electrocardiogram and modify the coefficients according to specific rules to eliminate motion artifacts. To automatically detect motion artifacts, they employed the electrode-skin impedance measured between two ECG electrodes. Strasser et al. [10] calculate the upper and lower thresholds for different levels of a Stationary Wavelet Transform (SWT) of the artifact contaminated ECG to separate useful cardiac content from artifacts. Nagai et al. [9] and Berwal et al. [11] have consequently revised this approach by modifying the thresholds and the reconstruction rules and with it improved the results. These approaches do, however, assume that the QRS-complex and the P- and T-wave can be successfully removed from the data. Moreover, they rely on detecting outliers in the data, that can be either caused by motion or by irregularly appearing pathological symptoms of cardiac diseases.

Blind Source Separation (BSS) techniques derive from unsupervised learning and aim at separating the sources of a heterogeneous mixing system. Independent Component Analysis (ICA) is the most prominent approach in removing artifacts from the ECG. He et al. [20] apply ICA to detect and remove noise and artifacts in ECG. Their approach is based on finding the statistically independent components in multi-lead ECG data and distinguishing between artifact and useful cardiac activity using the kurtosis. This approach has been continually refined in the past years [21]–[23]. However, ICA requires at least two ECG leads and artificially imposes independence on the artifact and the cardiac components in the signal. Berwal et al. [11] demonstrate the limitations of ICA in artifact removal. They illustrated that ICA separates independent sources in the ECG affected by Bending but was not able to map the artifacts on one component and the useful cardiac information on the other component. The motion artifacts were thus not successfully separated from the ECG and remained in the signal.

Recently, many researchers have investigated the capability of tensor-based approaches in Blind Source Separation. Lovenia et al. [24] combine Tensor Decomposition and Wavelet Transformation to remove speech artifacts from the electroencephalogram (EEG). They recorded a series of EEG from multiple subjects performing a specific speech-related task to induce artifacts in the EEG. Their results suggest that Canonical Polyadic Decomposition (CPD) outperformed previously published methods like the Independent Component Analysis. Goh et al. [25] combine Block Term Decomposition (BTD), and the Continuous Wavelet Transform (CWT) to remove a series of motion-related artifacts from the EEG. The authors used temporal and spatial features after applying Tensor Decomposition to detect and remove these artifacts. Thanh et al. [26] employ a non-negative Tucker Decomposition to extract features from the EEG and distinguish between epileptic and non-epileptic spikes.

He et al. [27] employ a tensor-based approach as preprocessing of a 12-lead ECG for subsequent classification by a Gaussian spectral clustering. Hoang et al. [28] use the Tucker Decomposition to decompose multi-lead ECG and feed resulting features into a Convolutive Neural Network (CNN) in order to classify Premature Ventricular Contraction (PVC) of the heart. Lilienthal et al. [12] employ tensor decomposition to factorize ECG data and extract motion patterns without the integration of any reference sensors. The approach was based on the Canonical Polyadic Decomposition, and a tensor composed of wavelet transformed ECG data. The extracted components were subsequently analyzed on their correlation to the motion patterns by considering the reference sensors employed. Padhy et al. [29] provide a more detailed discussion of tensor-based approaches for cardiac applications.

III. Data Factorization

The following section provides a brief introduction to multi-dimensional data factorization. We shall explain the application to two-dimensional structures and subsequently expand these models to the multi-dimensional data space.

A. Matrix Factorization

Matrix factorization belongs to a class of filtering algorithms that decompose a matrix into the product of lower-rank matrices. These techniques are commonly employed to extract latent information from the data that would otherwise remain hidden. Singular Value Decomposition (SVD) is one factorization technique that will subsequently be explained.

Assume we are given a matrix $\mathbf{X}$ with the dimensions $m \times n$. Applying the Singular Value Decomposition on this matrix factorizes it into the product of three lower-rank matrices $\mathbf{U}$, Σ and $\mathbf{V}$, according to the following Equation:

$$\mathbf{X} = \mathbf{U}\mathbf{\Sigma}\mathbf{V}^{\mathbf{T}} \tag{1}$$

where, $\mathbf{U}$ and $\mathbf{V}$ are the left, respective right singular matrices and,

- $\mathbf{U} \in \mathbb{R}^{m \times m}$ being an orthogonal matrix
- $\mathbf{\Sigma} \in \mathbb{R}^{m \times n}$ being a non-negative matrix, that is all zero except for diagnonal entries
- $\mathbf{V} \in \mathbb{R}^{n \times n}$ being an orthogonal matrix

The columns of $\mathbf{U}$ and $\mathbf{V}$ are orthonormal. The essential characteristics of Singular Value Decomposition are reflected in the structure of Σ. As described in Equation 2, its entries are arranged in descending order of the singular values σ_{ii}. These singular values reveal the number and the weight of the basic features that are hidden in $\mathbf{X}$.

$$\sigma_{11} \geq \sigma_{22} \geq ... \geq \sigma_{min(mn)} \tag{2}$$

The singular values can subsequently be the source of an exhaustive analysis of the data. By examining the number of singular values $\sigma_{ii} \gg 0$, we can identify a low-rank approximation of the initial matrix $\mathbf{X}$. An estimation of the initial matrix $\mathbf{X}$ can be calulated by only considering the first R singular values contributing to the data as follows, where the operator $\circ$ denotes the elementwise multiplication:

$$\mathbf{X} \approx \sum_{r=1}^{R} \sigma_{rr}\ \mathbf{u}_r \circ \mathbf{v}_r \tag{3}$$

As illustrated in Figure 1, the Singular Value Decomposition can be considered as a summation of R rank-one matrices. The decomposition of $\mathbf{X}$ can thus be viewed as an outer product of the left and right singular vectors $\mathbf{u}_r$ and $\mathbf{v}_r$, scaled by the respective singular value σ_r.

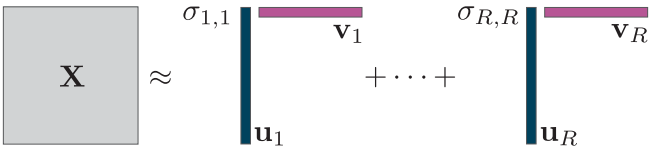

Fig. 1. The principle of Singular Value Decomposition.

Singular Value Decomposition is applicable only to data that can be expressed in terms of a matrix $\mathbf{X}$. However, when dealing with multi-channel sources, these dimensions are time and channel. This would hinder the analysis of hidden features in the frequency space. Therefore advanced processing techniques are required to handle the coherences in multi-dimensional data.

B. Tensor Decomposition

The following section presents a brief introduction to the basics of tensor decomposition. We will explain the Canonical Polyadic Decomposition (CPD), which we subsequently apply to remove motion artifacts from the ECG. Carroll and Chang [30] and Harshman [31] independently proposed the Canonical Polyadic Decomposition (CPD). For a more comprehensive analysis of tensor decomposition approaches, we refer the reader to the following review article [32].

Matrix factorization methods (e.g., Singular Value Decomposition (SVD), Independent Component Analysis (ICA)) factorize a matrix into a subset of smaller matrices. However, all matrix factorization techniques require constraints of the factors (i.e., orthogonality for SVD, independence for ICA) to decompose the data uniquely. These constraints are artificially imposed on the data and do not derive from the natural characteristics present in the ECG.

Similarly to matrix factorization, the concept of multi-dimensional decomposition techniques is to extract underlying or latent features from a given multi-dimensional array (an N-way tensor) $\mathcal{X}$. A three-way tensor is a three-dimensional array having $I \times J \times K$ elements:

$$\begin{aligned} \mathcal{X} &= \mathbf{a} \circ \mathbf{b} \circ \mathbf{c} \\ \mathcal{X} &\in \mathbb{R}^{I \times J \times K} \end{aligned} \tag{4}$$

The Canonical Polyadic Decomposition is a rank-based tensor decomposition that decomposes a given multi-dimensional tensor into a linear combination of rank-one tensors. Such rank-one tensor is also referred to as a pure tensor. Assuming we have a three-dimensional tensor, this tensor is of rank-one if it can be expressed as the tensor product of three vectors, as described in Equation 4. A subsequent analysis of each component of the rank-one tensors can accordingly uncover hidden features in the data. Unlike matrix decompositions, tensor decomposition can uniquely decompose a given n-dimensional dataset without imposing harsh constraints on the factors. However, the decomposition is based on the natural multi-linear relationship present in the data. The following Equation expresses this model for the three-dimensional case:

$$\mathcal{X} \approx \sum_{r=1}^{R} \mathbf{a}_r \circ \mathbf{b}_r \circ \mathbf{c}_r \tag{5}$$

where R is a natural number representing the quantity of rank-one components in the decomposition, also referred to as the decomposition rank. The resulting rank-one tensors consist of three loading vectors ($\mathbf{a}_i$, $\mathbf{b}_i$, and $\mathbf{c}_i$), one for each dimension of the initial tensor $\mathcal{X}$. Figure 2 demonstrates the principle of CPD for an R component model.

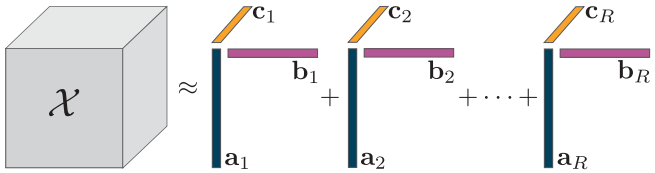

Fig. 2. The principle of Canonical Polyadic Decomposition for a three-dimensional tensor.

IV. Tensor Decomposition

A. Data acquisition

We acquired the wireless electrocardiogram and physical activity by employing the *Shimmer3* sensor platform [33]. This platform contains a 3D gyroscope, a 3D accelerometer, a chip to measure the bioimpedance, and a 5-lead WECG, which can be sampled synchronously.

To investigate the influence of motion on the electrocardiogram, we deployed two sensor setups to independently record the wireless electrocardiogram at rest as well as isolated motion artifacts at the back of the subjects. We intended to generate artificially disturbed ECG sequences.

Therefore, we placed one *Shimmer3* platform centrally on the sternum and attached two electrodes at the left and right arm position, resulting in the Einthoven lead I (LA-RA). An additional electrode at the right leg position served as reference potential (refer to Fig. 3). Thereby, we recorded the WECG at rest from 11 healthy subjects at a rate of 512 samples per second.

Noise recordings were obtained by placing one *Shimmer3* sensor at the back of each subject at the height of the lumbar curve. The bias electrode (B) was placed centrally on the spine. The reference electrode (R) was located approximately $3.5\,\mathrm{cm}$ to the right. The positive electrode (P) was positioned approximately $10\,\mathrm{cm}$ to the right of the bias electrode. All distances refer to the measurement between the electrodes' center. Figure 3 depicts the employed sensor setup for both placements. We calibrated the accelerometer to record accelerations of ± 16G, and the gyroscope to measure an angular velocity up to $500\,^\circ\,\mathrm{s}^{-1}$. These ranges are sufficient for all movements considered in our experimental setup.

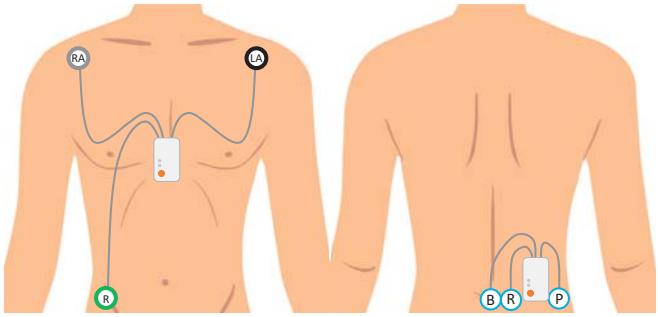

Fig. 3. Sensor placement at the front and the back.

Obtaining isolated noise recordings and generate artificially disturbed WECG sequences has previously been used to analyze the characteristics of motion artifacts and evaluate noise reduction performances on ECG signals [18], [34], [35]. The underlying assumption is that cardiac influence is negligible at the lumbar curve, and motion artifacts dominate the ECG. We have subsequently generated artificial motion artifact contaminated ECG by adding the noise recording on the clean data of the respective subject. All noise recordings were scaled to generate a Signal-to-Noise-Ratios (SNR) of $-5\,\mathrm{dB}$.

The advantage of this approach is the availability of a "ground-truth" signal - the clean ECG at rest. We can thus quantify the artifacts that the proposed approach removes from the WECG. In contrast to artificially generated motion artifacts (e.g., sinusoidal waves), we are more likely to capture the statistical properties and distinct characteristics of genuine motion artifacts. Moreover, reference sensors are available that help to characterize the artifacts in the data. Subsequently, we do not rely on secondary quantities (e.g., beat detection algorithms) to evaluate the performance of the motion artifact removal.

Table I contains all movements considered in our experimental setup. They were selected to reflect different aspects of everyday life, including motions of lower and higher intensity. We intentionally included movements of light intensity (e.g., Walking and Bending forward) as we associate these with elderly living. We tried to execute the movements under normal conditions. Only Bending forward, Standing up, and Jumping were performed on the spot. Because Running and Jumping are physically exhausting, these were conducted in four episodes of $30\,\mathrm{s}$ with $15\,\mathrm{s}$ of rest in between. We subsequently detected the active segments and removed the inactive periods from the dataset, resulting in signal lengths of $2\,\mathrm{min}$ for all activities.

TABLE I
OVERVIEW OF THE PHYSICAL ACTIVITIES.

No.	Movement Type	Duration in *mm:ss*
1	Stand up from chair and sit down	02:00
2	Bend forward and come up again	02:00
3	Walking	02:00
4	Running	02:45
5	Jumping on the spot	02:45
6	Stairs up and down	02:00

B. Preprocessing and Tensor construction

As the characteristics between the interfacing medium between the ECG electrodes and the patients' skin change continuously, the measurements are subject to a gradual drift in the baseline. Furthermore, high-frequency noise and powerline interference can additionally disturb the signal. To remove these distortions from the ECG, we applied digital frequency filters. All signals were preprocessed using a low-pass filter with a cutoff frequency of $f_{c,low} = 80\,\mathrm{Hz}$ and a high-pass filter with a cutoff frequency of $f_{c,high} = 0.5\,\mathrm{Hz}$. The cut-off frequencies applied are following the proposed sub-bands for ECG interpretation [36]. Figure 4 depicts a gradual drift in the baseline of the WECG and the preprocessed ECG data.

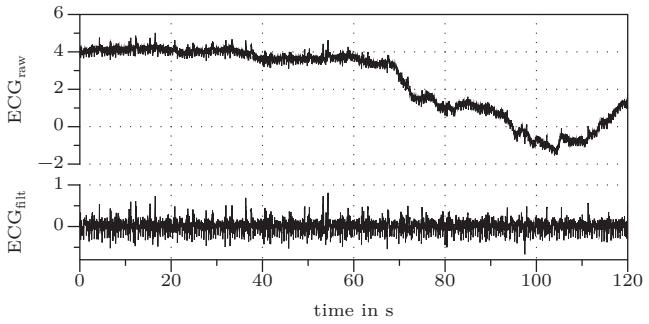

Fig. 4. Removal of baseline wander from the ECG using digital frequency filters.

Subsequently, we divided the recorded data ($t_d = 120\,\mathrm{s}$) into four episodes of $30\,\mathrm{s}$ for each subject. To avoid bias in the decomposition process, we normalized the data according to Equation 6. Normalization is a common practice to give the input data from heterogeneous sources equal statistical weight [37].

$$x_{norm}(t) = \frac{x(t) - \min(x)}{\max(x) - \min(x)} \tag{6}$$

A variety of time-frequency transformations are available to capture temporal and spectral aspects of the data simultaneously (e.g., Short-Time Fourier Transform (STFT) [38],

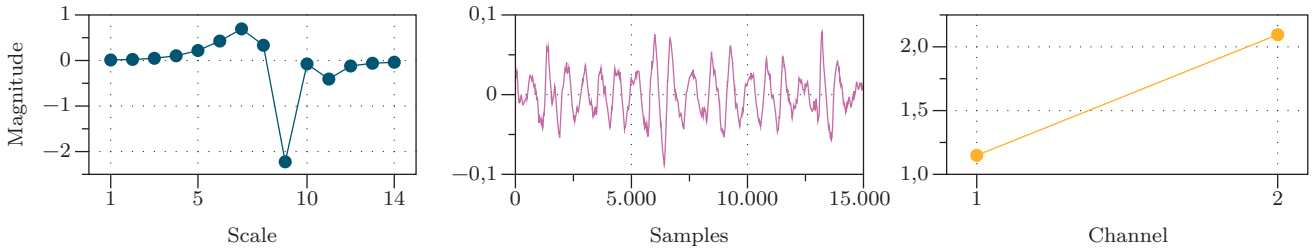

Fig. 5. The result of a rank five CPD for Bending using the accelerometer, including the components for scale, samples and channel.

and Wavelet Transformations (Discrete Wavelet Transform (DWT), and Continuous Wavelet Transform (CWT) [39]). Fourier Transformations can model changes in the spectral characteristics but are incapable of detecting the moment when these changes occur. The Short-Time Fourier Transform (STFT) segments the data into multiple windows and applies the Fast-Fourier Transform in each of them. Thereby the frequency components in that specific time window can be determined. However, the spectral and temporal resolution are conflicting. STFT can achieve a good time resolution by using small windows to calculate the Fourier Transform, but this inevitably results in poor spectral resolution. Choosing the appropriate window length is thus a trade-off between time and frequency resolution.

Wavelet transformations apply a base function Ψ, which is compressed or stretched to capture high- or low-frequency components in the data. The advantage of wavelet transformations is the excellent time resolution for high frequencies while preserving a high-frequency resolution for low frequencies. It is, therefore, suitable to capture the temporal and spectral aspects of motion artifacts and cardiac data adequately. This transformation has been used extensively in the reduction of artifacts from the ECG and other biomedical applications in recently [3], [37], [40].

We employed the Stationary Wavelet Transform (SWT), otherwise known as Maximal Overlap Discrete Wavelet Transform (MODWT) [41], to transform the ECG and motion reference data into the time-frequency space. In contrast to the regular DWT, the output of each level of SWT contains the same number of samples as the input data enabling us to construct a tensor with a consistent number of samples for each wavelet decomposition stage. As a mother wavelet, we selected the Haar wavelet [42]. During the wavelet transformation, this mother wavelet is scaled to cover different frequency bands of the data. The scaling parameter is inversely proportional to the frequency: A high scale stretches the mother wavelet and represents low frequencies of the signal while a low scale compresses the wavelet resulting in covering the higher frequencies of the signal. The MODWT transforms the WECG and reference data into 14 scales, each representing different frequency bands in the signal.

Each sensor generates a one-dimensional time-related vector of size J, where J refers to the number of samples. We transformed the data using Stationary Wavelet Transform into a two-dimensional frequency-time matrix of size $I \times J$, where I refers to the wavelet scales and is inversely proportional to the frequency. By combining the wavelet transformed data from the WECG and one motion reference sensor in a multi-dimensional array, we constructed a tensor of dimensions $I \times J \times K$ (see Fig. 6). The frontal slice of the tensor represents the wavelet decomposed data of one sensor. For each segment recorded, we selected the accelerometer/gyroscope axis that correlates best with the respective artifactual ECG.

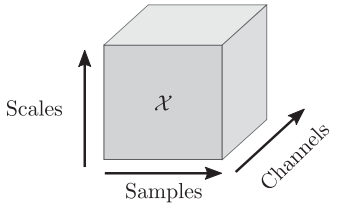

Fig. 6. Construction of the three-dimensional tensor combing the WECG and a reference sensor.

C. Tensor Decomposition and Reconstruction

After constructing the tensor, we applied a five component Canonical Polyadic Decomposition according to Equation 5. For all subsequent tensor modelling, we employed the *Tensorlab 3.0* Toolbox in *MATLAB 2019b* [43].

The decomposed data contains three loading vectors, each corresponding to one dimension of the initial tensor $\mathcal{X}$. Fig. 5 illustrates these loading vectors for one factor resulting from a Canonical Polyadic Decomposition applied to a three-dimensional tensor. The first loading vector represents the distribution of the corresponding data among the wavelet scales. The scales thereby result from the MODWT. The magnitude encodes the strength of the CPD-factor in the respective frequency band. The second loading vector represents the temporal features, i.e. the temporal distribution of the factor. The third vector represents the distribution of the latent factor among the two channels employed in the decomposition process (i.e., accelerometer (Ch. 1) and WECG (Ch. 2)). It encodes the magnitude of the CPD-factor among the channels, i.e. how strong the respective component is present in Ch.1/Ch.2. The following list illustrates the necessary steps in denoising the WECG.

The basic premise of our attempt is that latent factors correlating to motion artifacts manifest themselves in the ECG

Algorithm 1: CPD Artifact Reduction

Data: ecg, motion_reference
Result: denoised ecg

```
Frequency Filter;
Normalization;
Wavelet Transform;
Tensor Construction;
Tensor Decomposition;
Reconstruction from CPD-Model;
Inverse Wavelet Transform;
Artifact Reduction of ECG (see Eq. 7);
```

and the motion reference. Subsequently, applying the tensor decomposition with a reference sensor as an additional source of information can take advantage of the correlation between the input data and extract motion artifacts from the WECG. A reconstruction of the decomposed tensor and the inverse wavelet decomposition leads to the components which are present in both sensors (the ECG and the inertial reference). The noise-free ECG signal is subsequently obtained by subtracting the artifact estimation from the noisy ECG as follows:

$$\mathrm{ECG}_{clean,est.} = \mathrm{ECG}_{noisy} - \mathrm{Artifact}_{est.,cpd} \tag{7}$$

V. Evaluation

The following section provides insights into the findings we obtained by combing the WECG and the inertial data using CPD to remove motion artifacts. To objectively evaluate the approach, we calculated the Signal-to-Noise Ratio (SNR) as described in Equation 8.

$$\mathrm{SNR} = 10\ \lg(\frac{P_{\mathrm{Signal}}}{P_{\mathrm{Artifact}}})\mathrm{dB} \tag{8}$$

where P_{Signal} is the power of the noise-free ECG and P_{Artifact} is the power of the original, respectively remaining, motion artifact in the ECG after noise reduction. Secondly, we determined the Pearson correlation coefficient R between the motion reference accelerometer and the ECG before and after noise reduction. This will provide insights into how well the CPD-model removes mutual information from the ECG.

In addition to the Signal-to-Noise Ratio we evaluated the performance by considering the Root Mean Squared Error (RMSE) between the artifacts estimated by the CPD y_{est} and the original artifacts y_{true}. The RMSE for two signals of length n is defined as follows:

$$\mathrm{RMSE} = \sqrt{(\frac{1}{n})\sum_{i=1}^{n}(y_{est} - y_{true})^2} \tag{9}$$

Table II contains the results of removing motion artifacts from the ECG using the CPD-model and the accelerometer. All values refer to the median from the 11 subjects participating in the study. We only regarded the absolute values of the Pearson correlation coefficient, to validate if and how strong the accelerometer and the ECG are correlated after noise reduction.

TABLE II
Performance of the Canonical Polyadic Decomposition to remove motion artifacts using the accelerometer.

Movement	$\mathrm{SNR}_{\mathrm{after}}$ in dB	$\mathrm{RMSE}_{\mathrm{Artifact}}$	$\mathrm{R}_{\mathrm{Ref,before}}$	$\mathrm{R}_{\mathrm{Ref,after}}$
Jumping	1.1	0.07	0.23	0.05
Running	1.1	0.06	0.21	0.06
Bending	2.4	0.06	0.27	0.02
Standing up	1.1	0.06	0.12	0.05
Stairs	0.5	0.06	0.14	0.05
Walking	0.8	0.07	0.23	0.05

The CPD-model removes the most substantial portion of the motion artifacts and increases the Signal-to-Noise-Ration from $-5\,\mathrm{dB}$ to at least $0.5\,\mathrm{dB}$ for all movements regarded. There are, however, fine-grained differences in how well the algorithm performs for specific movements. When we regard the Signal-to-Noise-Ratio, the algorithm performs best for Bending forward and weaker for Climbing up and down a flight of stairs. For the remaining movements, the algorithm produces comparable levels of SNR.

Using the Canonical Polyadic Decomposition, we can effectively decrease the correlation between the ECG and the accelerometer R_{Ref} for all movements regarded in our analysis. Moreover, the Root Mean Squared Error (RMSE) between the original and the removed artifacts is low. We thereby infer that CPD can serve as a useful method to remove motion artifacts from the ECG.

We subsequently replaced the accelerometer in the third-order tensor with the gyroscope and the bioimpedance and repeated the decomposition and reconstruction procedure for each sensor separately. Figure 7 depicts the results in the form of the Signal-to-Noise-Ratio. Combing the ECG and the reference sensors significantly enhances the signal quality for all sensors types. Overall, the accelerometer performs the best for all movements save Bending forward. There are fine-grained differences in how well the respective sensors remove artifacts for a specific movement. Nevertheless, all sensors can be employed in the proposed tensor-based approach.

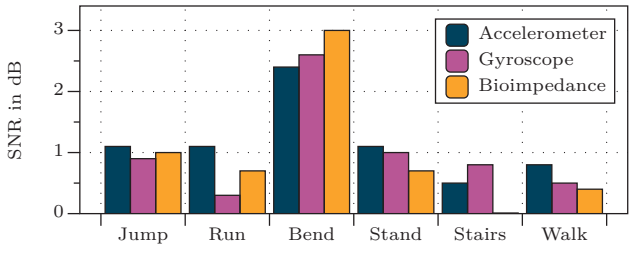

Fig. 7. Performance of the CPD-model for different reference sensors.

To illustrate the performance of the artifact reduction method, Figure 8 displays the results of our proposed approach for a $30\,\mathrm{s}$ interval of Bending forward. Note that the

difference in magnitude of ECG_{noisy} and ECG_{est} results from the removal of the mean in the decomposition process. The signal ECG_{noisy} is significantly disturbed due to the artificially generated motion artifacts. Not all QRS-complexes are visually detectable, and significant noise affects all parts of the ECG. After applying the proposed tensor approach, we can remove the majority of motion artifacts from the ECG. The QRS-complexes become visible, and even the P-waves can now be manually detected.

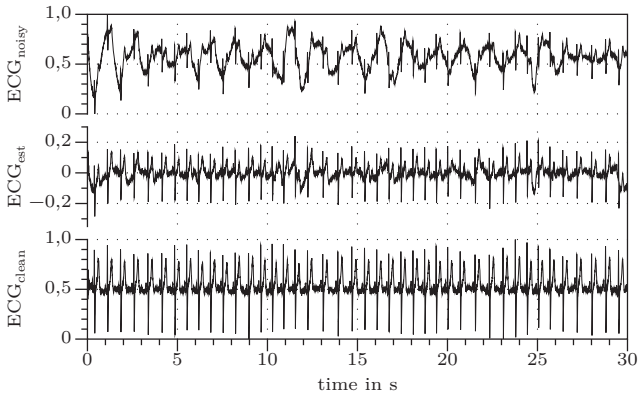

Fig. 8. Performance of the CPD motion artifact reduction for one subject performing the movement Bending.

We subsequently compare the removed and the original artifacts as well as the accelerometer as motion reference in Fig. 9. The artifacts extracted using the CPD approach relate to the artifacts induced. Moreover, the extracted artifacts from the ECG do not contain any apparent cardiac information (e.g., QRS-complexes). This is especially vital as applying motion artifact reduction should not change the characteristics of the underlying ECG and remove valuable information.

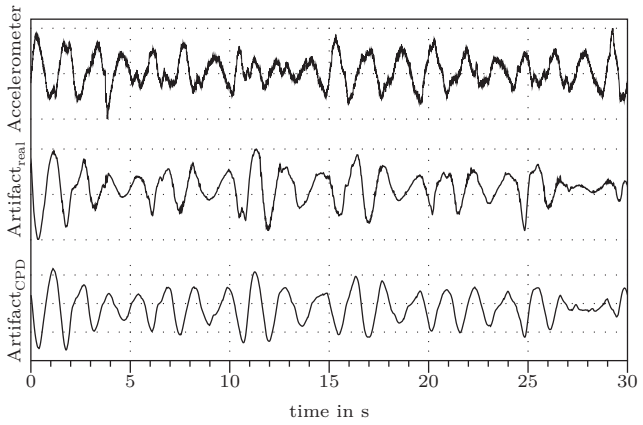

Fig. 9. Comparison of the accelerometer, the original artifacts and the extracted artifacts using the proposed CPD-model for one subject performing the movement Bending.

VI. Conclusion and Future Work

In this paper, we employed the Canonical Polyadic Decomposition to remove motion artifacts from the measurements of a wireless electrocardiogram. We recorded data from 11 healthy subjects undertaking various types of movements associated with everyday activities. The movement types were chosen to reflect different aspects of daily routines and cover intensities associated with elderly living. Using the *Shimmer3* platform, we employed an additional wireless ECG at the back of the subjects to record motion artifacts with as little cardiac content as possible. These noise measurements were subsequently scaled and added to a noise-free ECG of the respective subject in rest. Thereby we generated ECG with artificially superimposed motion artifacts.

We constructed a three-dimensional tensor consisting of one ECG lead and one of the available reference sensors (accelerometer, gyroscope, and bioimpedance). By employing the Canonical Polyadic Decomposition, we combined the data and extracted mutual information present in the ECG and the motion reference sensor. These were subsequentially subtracted from the ECG to obtain noise-free data. The results suggest that CPD can successfully remove motion artifacts generated by a variety of different movements. All of the regarded movement sensors are capable of capturing artifacts and can be included in the multi-dimensional tensor. We conclude that CPD is a powerful tool to remove motion artifacts from the ECG without additionally disturbing the signal or removing useful cardiac information.

In future research, the authors intend to closely investigate the correlation between the ECG and motion artifacts, as this will likely influence the outcome of the decomposition process. These data will help to characterize the motion artifacts better and thereby enhance the quality of the decomposition process. Our approach was limited to the Canonical Polyadic Decomposition. Advanced tensor methods such as Block Term Decomposition or Tucker Decomposition might improve the performance of the motion artifact reduction technique as these methods offer more relaxed constraints in the decomposition process.

References

[1] World Health Organization, "Global Health Estimates 2016: Deaths by Cause, Age, Sex, by Country and by Region, 2000-2016," World Health Organization, Geneva, Tech. Rep., 2018.

[2] N. V. Thakor, J. G. Webster, and W. J. Tompkins, "Estimation of QRS Complex Power Spectra for Design of a QRS Filter," *IEEE Transactions on Biomedical Engineering*, vol. BME-31, no. 11, pp. 702–706, nov 1984.

[3] M. Kirst, B. Glauner, and J. Ottenbacher, "Using DWT for ECG motion artifact reduction with noise-correlating signals," in *Annual International Conference of the IEEE Engineering in Medicine and Biology Society*. IEEE, aug 2011, pp. 4804–4807.

[4] P. Mishra and S. K. Singla, "Artifact Removal from Biosignal using Fixed Point ICA Algorithm for Pre-processing in Biometric Recognition," *Measurement Science Review*, vol. 13, no. 1, pp. 7–11, jan 2013.

[5] H. Kwon, S. Oh, and V. K. Varadan, "Motion artifact removal algorithm by ICA for e-bra: a women ECG measurement system," in *Nanosensors, Biosensors, and Info-Tech Sensors and Systems 2013*, V. K. Varadan, Ed., vol. 8691, no. April 2013, apr 2013, p. 86910A.

[6] T. Alkhidir, A. Sluzek, and M. K. Yapici, "Simple method for adaptive filtering of motion artifacts in E-textile wearable ECG sensors," *Proceedings of the Annual International Conference of the IEEE Engineering in Medicine and Biology Society, EMBS*, vol. 2015-Novem, pp. 3807–3810, 2015.

[7] K. Hyejung, K. Sunyoung, N. Van Helleputte, T. Berset, G. Di, I. Romero, J. Penders, C. Van Hoof, and R. F. Yazicioglu, "Motion artifact removal using cascade adaptive filtering for ambulatory ECG monitoring system," in *2012 IEEE Biomedical Circuits and Systems Conference (BioCAS)*. IEEE, nov 2012, pp. 160–163.

[8] D. Tong, K. Bartels, and K. Honeyager, "Adaptive reduction of motion artifact in the electrocardiogram," in *Proceedings of the Second Joint 24th Annual Conference and the Annual Fall Meeting of the Biomedical Engineering Society] [Engineering in Medicine and Biology*, vol. 2, no. February. IEEE, 2002, pp. 1403–1404.

[9] S. Nagai, D. Anzai, and J. Wang, "Motion artefact removals for wearable ECG using stationary wavelet transform," *Healthcare Technology Letters*, vol. 4, no. 4, pp. 138–141, aug 2017.

[10] F. Strasser, M. Muma, and A. M. Zoubir, "Motion artifact removal in ECG signals using multi-resolution thresholding," *European Signal Processing Conference*, no. Eusipco, pp. 899–903, 2012.

[11] D. Berwal, V. C. R., S. Dewan, J. C. V., and M. S. Baghini, "Motion Artifact Removal in Ambulatory ECG Signal for Heart Rate Variability Analysis," *IEEE Sensors Journal*, vol. 19, no. 24, pp. 12 432–12 442, dec 2019.

[12] J. Lilienthal and W. Dargie, "Extraction of Motion Artifacts from the Measurements of a Wireless Electrocardiogram using Tensor Decomposition," *International Conference on Information Fusion*, 2019.

[13] S. Poungponsri and X. H. Yu, "An adaptive filtering approach for electrocardiogram (ECG) signal noise reduction using neural networks," *Neurocomputing*, vol. 117, pp. 206–213, 2013.

[14] X. Xu, Y. Liang, P. He, and J. Yang, "Adaptive Motion Artifact Reduction Based on Empirical Wavelet Transform and Wavelet Thresholding for the Non-Contact ECG Monitoring Systems," *Sensors*, vol. 19, no. 13, p. 2916, jul 2019.

[15] Xiong, Chen, and Huang, "A Wavelet Adaptive Cancellation Algorithm Based on Multi-Inertial Sensors for the Reduction of Motion Artifacts in Ambulatory ECGs," *Sensors*, vol. 20, no. 4, p. 970, feb 2020.

[16] K. T. Sweeney, T. E. Ward, and S. F. McLoone, "Artifact removal in physiological signals-practices and possibilities," *IEEE Transactions on Information Technology in Biomedicine*, vol. 16, no. 3, pp. 488–500, may 2012.

[17] Y. Liu and M. G. Pecht, "Reduction of skin stretch induced motion artifacts in electrocardiogram monitoring using adaptive filtering," *Annual International Conference of the IEEE Engineering in Medicine and Biology - Proceedings*, pp. 6045–6048, 2006.

[18] I. Romero, D. Geng, and T. Berset, "Adaptive filtering in ECG denoising: A comparative study," *Computing in Cardiology*, vol. 39, pp. 45–48, 2012.

[19] F. A. Ghaleb, M. B. Kamat, M. Salleh, M. F. Rohani, and S. Abd Razak, "Two-stage motion artefact reduction algorithm for electrocardiogram using weighted adaptive noise cancelling and recursive Hampel filter," *PLOS ONE*, vol. 13, no. 11, nov 2018.

[20] T. He, G. Clifford, and L. Tarassenko, "Application of independent component analysis in removing artefacts from the electrocardiogram," *Neural Computing and Applications*, vol. 15, no. 2, pp. 105–116, apr 2006.

[21] M. Milanesi, N. Martini, N. Vanello, V. Positano, M. F. Santarelli, and L. Landini, "Independent component analysis applied to the removal of motion artifacts from electrocardiographic signals," *Medical & Biological Engineering & Computing*, vol. 46, no. 3, pp. 251–261, mar 2008.

[22] A. Hyvärinen, "Independent component analysis: Recent advances," *Philosophical Transactions of the Royal Society A: Mathematical, Physical and Engineering Sciences*, vol. 371, no. 1984, pp. 20 110 534–20 110 534, 2013.

[23] J. Kuzilek, V. Kremen, F. Soucek, and L. Lhotska, "Independent component analysis and decision trees for ECG holter recording de-noising," *PLoS ONE*, vol. 9, no. 6, p. e98450, jun 2014.

[24] H. Lovenia, H. Tanaka, S. Sakti, A. Purwarianti, and S. Nakamura, "Speech Artifact Removal from Eeg Recordings of Spoken Word Production with Tensor Decomposition," in *ICASSP 2019 - 2019 IEEE International Conference on Acoustics, Speech and Signal Processing (ICASSP)*. IEEE, may 2019, pp. 1115–1119.

[25] S. K. Goh, H. A. Abbass, K. C. Tan, A. Al-Mamun, C. Guan, and C. C. Wang, "Multiway analysis of EEG artifacts based on Block Term Decomposition," *Proceedings of the International Joint Conference on Neural Networks*, vol. 2016-Octob, pp. 913–920, 2016.

[26] L. T. Thanh, N. T. A. Dao, N. V. Dung, N. L. Trung, and K. Abed-Meraim, "Multi-channel EEG epileptic spike detection by a new method of tensor decomposition," *Journal of Neural Engineering*, vol. 17, no. 1, p. 016023, jan 2020.

[27] H. He, Y. Tan, and J. Xing, "Unsupervised classification of 12-lead ECG signals using wavelet tensor decomposition and two-dimensional Gaussian spectral clustering," *Knowledge-Based Systems*, vol. 163, pp. 392–403, jan 2019.

[28] T. Hoang, N. Fahier, and W.-C. Fang, "Multi-Leads ECG Premature Ventricular Contraction Detection using Tensor Decomposition and Convolutional Neural Network," in *2019 IEEE Biomedical Circuits and Systems Conference (BioCAS)*. IEEE, oct 2019, pp. 1–4.

[29] S. Padhy, G. Goovaerts, M. Boussé, L. De Lathauwer, and S. Van Huffel, "The Power of Tensor-Based Approaches in Cardiac Applications," 2020, pp. 291–323.

[30] J. D. Carroll and J. J. Chang, "Analysis of individual differences in multidimensional scaling via an n-way generalization of "Eckart-Young" decomposition," *Psychometrika*, vol. 35, no. 3, pp. 283–319, sep 1970.

[31] R. A.Harshman, "Foundations of the PARAFAC procedure: Models and conditions for an "explanatory" multimodal factor analysis," *UCLA Working Papers in Phonetics*, vol. 16, no. 10, pp. 1–84, sep 1970.

[32] T. G. Kolda and B. W. Bader, "Tensor decompositions and applications," *SIAM Review*, vol. 51, no. 3, pp. 455–500, aug 2009.

[33] A. Burns, B. R. Greene, M. J. McGrath, T. J. O'Shea, B. Kuris, S. M. Ayer, F. Stroiescu, and V. Cionca, "SHIMMER™ – A Wireless Sensor Platform for Noninvasive Biomedical Research," *IEEE Sensors Journal*, vol. 10, no. 9, pp. 1527–1534, sep 2010.

[34] D. Buxi, S. Kim, N. Van Helleputte, M. Altini, J. Wijsman, R. F. Yazicioglu, J. Penders, and C. Van Hoof, "Correlation between electrode-tissue impedance and motion artifact in biopotential recordings," *IEEE Sensors Journal*, vol. 12, no. 12, pp. 3373–3383, 2012.

[35] I. Romero, "PCA and ICA applied to noise reduction in multi-lead ECG," *Computing in Cardiology*, vol. 38, pp. 613–616, 2011.

[36] J. W. Mason, E. W. Hancock, and L. S. Gettes, "Recommendations for the Standardization and Interpretation of the Electrocardiogram," *Circulation*, vol. 115, no. 10, pp. 1325–1332, 2007.

[37] E. Acar, C. Aykut-Bingol, H. Bingol, R. Bro, and B. Yener, "Multiway analysis of epilepsy tensors," *Bioinformatics*, vol. 23, no. 13, pp. 10–18, 2007.

[38] J. B. Allen, "Short Term Spectral Analysis, Synthesis, and Modification by Discrete Fourier Transform," *IEEE Transactions on Acoustics, Speech, and Signal Processing*, vol. 25, no. 3, pp. 235–238, jun 1977.

[39] C. E. Heil and D. F. Walnut, "Continuous and discrete wavelet transforms," *SIAM Review*, vol. 31, no. 4, pp. 628–666, dec 1989.

[40] J. E. Kline, H. J. Huang, K. L. Snyder, and D. P. Ferris, "Isolating gait-related movement artifacts in electroencephalography during human walking," *Journal of Neural Engineering*, vol. 12, no. 4, 2015.

[41] D. B. Percival, A. T. Walden, D. B. Percival, and A. T. Walden, "The Maximal Overlap Discrete WaveletTransform," in *Wavelet Methods for Time SeriesAnalysis*. Cambridge: Cambridge University Press, 2013, no. May, pp. 159–205.

[42] A. Haar, "Zur Theorie der orthogonalen Funktionensysteme," *Mathematische Annalen*, vol. 71, no. 1, pp. 38–53, mar 1911.

[43] N. Vervliet, O. Debals, L. Sorber, M. Van Barel, and L. De Lathauwer, "Tensorlab 3.0," 2016. [Online]. Available: https://www.tensorlab.net